Microstructure and Wetting Performance of High-Pressure Cold Sprayed Quasi-Crystalline Composite Coatings

R. Jafari, J. Kiilakoski, M. Honkanen, M. Vippola, H. Koivuluoto

High-pressure cold spraying has shown significant potential in manufacturing metallic composite coatings for a wide range of industrial applications, including wear and corrosion protection. Quasi-crystalline materials, in turn, are promising candidates due to their unique microstructural features. Combining these concepts, metallic composite coatings were generated using high-pressure cold spraying to produce functional and protective coatings. Several spray trials were done to detect the effect of compositions and size of quasi-crystalline feedstock materials mixed with metal powders, Al6061, and stainless steel 316L, on coating microstructure, integrity, and surface properties. A scanning electron microscope was used to examine the microstructure of the feedstock materials and composite coatings. A 3D surface optical profilometer was also used to investigate surface texture. The wettability of the coating surfaces was measured by static water contact angles using a droplet shape analyzer. Cold-sprayed quasi-crystalline composite coatings showed denser and well-integrated deposits with a random distribution of phases across the composite surface, indicating promising structural reliability and hydrophobic behavior.

1 Introduction

In many industrial sections, operational challenges exist when a component is in contact with water in the working condition. Corrosion, fouling, current leakage, and heat transfer efficiency reduction, to name a few, are examples of such complications that can be avoided or reduced by employing hydrophobic coatings. By virtue of the low wetting feature, hydrophobic coatings can reduce water droplet contact and adhesion, interrupting unwanted interactions with water and species in water. Acknowledging immense potential applications, there has been an increasing interest in developing durable hydrophobic coatings in both academic research and industrial fields [1,2].
Wetting behavior generally involves measuring water droplet contact angle (CA), which is defined as the angle between the water-air interface tangent and the water-solid interface. Surfaces with the contact angles of 90°<CA<150° are considered as hydrophobic, while higher and lower contact angles are placed in the categories of superhydrophobic and hydrophilic, respectively [3]. Using low surface energy materials and altering the surface roughness are effective strategies to fabricate water-repellant surfaces. However, the durability of most effective candidates generally made through thin layer modification of surfaces, nanotextured surfaces, polymeric, or fragile oxide layers are limited [4,5]. On the other hand, metals and metal alloys like Fe and Al-based alloys as conventional materials in most industries merely show hydrophilic behavior[6–8].
Quasi-crystalline materials with specific lattice structures have their own physical and chemical properties different from well-known crystalline networks [9]. Concerning research on properties of quasi-crystalline materials, they have shown low surface energy and other beneficial properties like low friction coefficient, low conductivity, considerable hardness, and corrosion protective behavior [10–13]. Therefore, they can be considered as a potential material for the fabrication of hydrophobic surfaces.
Thermal spray technologies with extensive possibilities can deposit versatile coating materials from soft polymeric materials to hard, brittle ceramics. Although thermal spray processes like High-Velocity Oxygen Fuel (HVOF) and plasma spray have been successfully employed in the deposition of hard and brittle quasi-crystalline powders, the phase change during the high-temperature deposition is inevitable [14,15]. Therefore, cold spraying with a significantly lower process temperature can preserve the valuable phases in initial feedstock, critical elements and desired properties [16]. In the current research, the effort was to incorporate micron-sized quasi-crystalline (QC) powders into metallic coatings to alter their wetting performance towards hydrophobicity. Coatings were produced by using pre-mixed Al-based QC powders and metallic powders with a high-pressure cold spray system. Surface features including topography, surface roughness and water droplet contact angles and of the coatings were studied to evaluate surface properties of these QC-based composites compared to metallic coatings.

2 Experimental Procedure

Feedstock materials and coating process:
In order to deposit the coatings, three different powder compositions were selected with the following specifications: gas atomized aluminium alloy (Al6061, 10-40 µm) supplied by TLS Technik (Germany), stainless steel (SS316L, PG-AMP-1010, 10-45µm) commercially available from Dycomet (The Netherlands), and two different size range of quasi-crystalline Al-based powders (Cristome A1 with a nominal composition of Al53.9-Fe13.8-Cr15.5-Cu17.5 wt%, 10-30 µm called as fine and 20-70 µm named as coarse, hereafter) supplied by Saint-Gobain Coating Solutions (France). A high-pressure cold spray system, PCS-100 (Plasma Giken Co., Ltd., Japan), mounted on an ABB robot arm (ABB Ltd., Finland), with nitrogen as the propeller gas was used to deposit coatings. A plastic nozzle for Al-based coatings and a hard metal nozzle for steel-based coatings were used. The cold spray process parameters for each coating can be found in Table 1. For the composite coatings, the desired portion of each component was mixed in a container and physically blended. All substrates were degreased with ethanol and grit blasted

using alumina grits (Mesh 40) prior to spraying the samples. A heating plate was positioned behind the substrate in a few of the trials, allowing to stabilize the surface temperature of the substrate prior to starting the spray process. This approach was decided based on the preliminary trials showing the influences of in-situ heat treatment on the microstructure and coatings performance.

Table 1. Sample codes, feedstock materials, process parameters and substrates used for cold spray coating production

Code	Feedstock Materials	Process parameters							
		P (bar)	T (°C)	SoD (mm)	Step (mm)	Feed (rpm)	Speed (m/ min)	lay-ers	Substrate
Al	Al6061	20	450	40	1.5	3	5	3	Al 6082
Al (HP) *	Al6061	20	450	40	1.5	3	5	3	Al 6082
SS	SS316L	50	900	40	1	2	10	2	Low carbon steel (S235)
Al25-fQC**	25 vol% Al6061 +QC A1 ***10-30*** *µm*	20	450	40	1.5	3	5	3	Al 6082
Al25-fQC (HP)	25 vol% Al6061 +QC A1 ***10-30*** *µm*	20	450	40	1.5	3	5	3	Al 6082
Al10-cQC***	10 vol% Al6061 +QC A1 ***20-70*** *µm*	20	450	40	1.5	3	5	3	Al 6082
Al50-cQC(HP)	50 vol% Al6061 +QC A1 **20-70** µm	20	450	40	1.5	3	5	3	Al 6082
SS25-cQC(HP)	25 vol% SS316L +QC A1 **20-70 µm**	50	900	40	1	2	10	3	Low carbon steel (S235)

* Heat plate temperature 300, sensed temperature: Al-a and Fe-based substrate were 200 and 250 °C respectively
** fine quasi-crystalline powders
*** coarse quasi-crystalline powders

Characterization

A topography of powders and coatings was investigated using a scanning electron microscope (SEM) (JEOL-IT500, Japan), operating at a 15 kV accelerating voltage. Secondary (SEs) and backscattered electrons (BSEs) detectors (shadowing (BSE-S) mode) were used to characterize the microstructure. The shadowing mode can concurrently accentuate compositional contrast and topographical characteristics, which are highly informative for composites. A sample of each coating was cut through the cross-section using a precision cutter and then hot mounted, ground, and polished to a mirror finish to validate the deposition of the coating using BSEs imaging in the SEM. ImageJ software package was used to measure the thickness via at least 10 individual measurements. Surface textures and associated parameters including S_a (surface arithmetic mean height, µm), S_q (root-mean-square height, µm) S_{sk} (skewness value) and S_{ku} (kurtosis value) were retrieved from a 2*2 cm^2 area scanned using the Alicona InfiniteFocus G5 optical 3D profilometer (Alicona Imaging GmbH, Austria) and processed in the IF-MeasureSuite V 5.1.

Droplet shape analysis (DSA)

Static contact angles (CA) measurements were performed at room temperature 23.5 °C ± 1 °C, and relative humidity equals 60 % ± 2 % using a droplet shape analyzer system (DSA100, Krüss, Germany). The procedure was consisted of releasing a 5 µl droplet MilliQ ultra-high purity water (Millipore Corporation, United States) over the coating surface. Before measurements, samples were cleaned with ethanol in an ultrasonic bath for 3 minutes to remove surface contamination and dried by air flow to accelerate the evaporation of ethanol from the surface. Samples were kept in a desiccator cabinet for one day to assure removal of water content trapped in the coatings and overnight in the controlled condition room. The contact angle made by the tangent of the air-water interface and the coating–water interface was recorded by the camera and estimated for at least 6 measurements in the automatic procedure. For the surfaces with a higher deviation in droplet contact angle over the surface, the number of trials was extended to 15 to reflect average behavior. Standard deviation was measured for each measurement set to consider the distribution of results.

3 Results

Powder morphology

Figure 1 represents the morphology of feedstock powders. Despite their size differences between coarse (Figure 1a) and fine (Figure 1b) quasi-crystalline (QC) powders, their geometry is close to spherical. An analogous texture can be seen on QC powders surfaces. Sporadic presence of satellites, small particles attached to main powders, can be observed in both distributions. Gas atomized Al6061 powder particles were spherical (Figure 1c), with smoother surface texture and more satellites attached to larger powders compared to QCs. Both QC and

Al6061 have several irregular particles marked with arrows in Figure 1(a-c), while the primary morphology of SS316L powder in Figure 1d is irregular in general due to the powder manufacturing method.

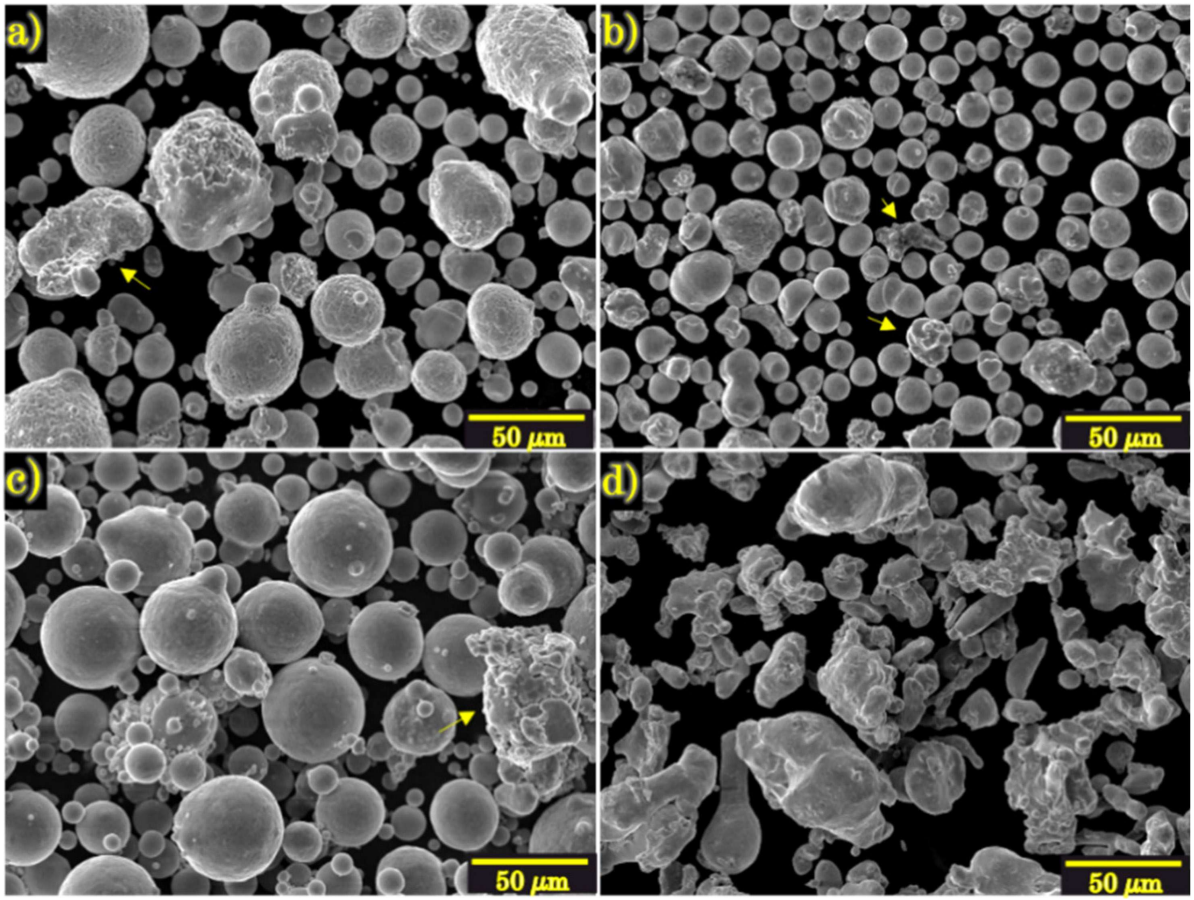

Figure 1. SEM-SE images of powder morphologies of a) coarse quasi-crystalline, b) fine quasi-crystalline, c) Al6061, and d) Stainless steel 316L powders.

Structural details and water droplet contact angle

Figure 2 shows two examples of features observed from the cross-section of the coatings Al6061 (a) and the coating consisting of an initial feedstock mixture of fine QC and 10 vol% Al6061 (b). Cold sprayed Al coating had high coating thickness due to the high deposition efficiency of ductile Al particle but (514 µm ± 78 µm), but disconnected pores can be seen through the cross-section, especially closer to the surface where the hammering effect from subsequently impacted particles is marginal [17]. According to Figure 2b a denser coating with an almost homogenous distribution of both QC and Al6061 particles could be noticed. Achieving such an improvement in structure, given the fact that spray parameters were the same, it shows the positive effect of QC particles in densification of the coating. Comparably, deposition efficiency was lower for the composite coating (coating thickness of 298 µm ± 24 µm), and the contribution of QC powders to the coating formation was lower than the initial feedstock blend. Interestingly, QC and Al particles appeared at the surface, perceived from higher magnification in Figure 2b. Since the hydrophobicity phenomenon is generally concerned with the surface properties, this paper focuses on surface characteristics of the coatings.

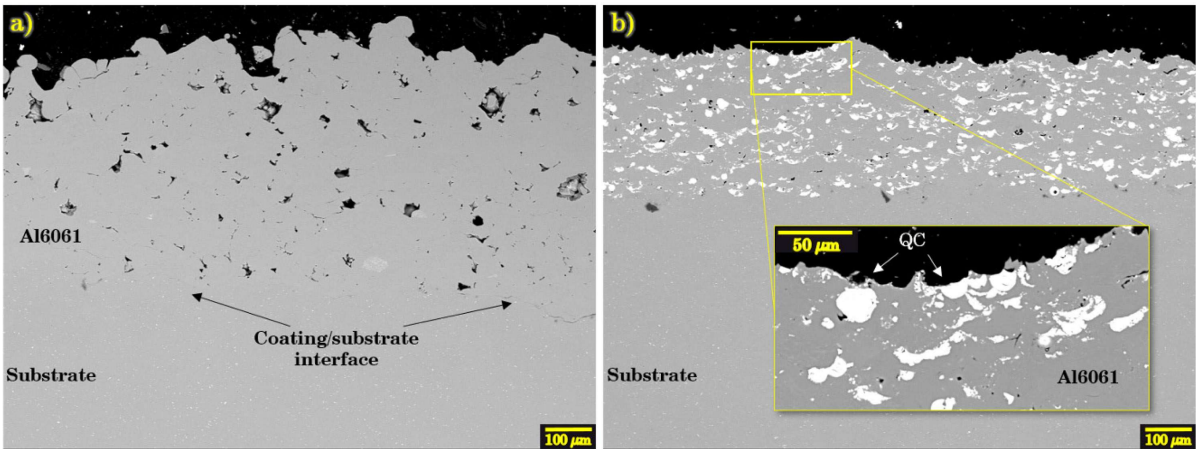

Figure 2. SEM-BSE images of coating cross-sections of cold sprayed a) Al and b) Al10-fQC coatings.

Almost similar surface topography was observed from the cold sprayed Al6061 coatings regardless of heating condition of the substrate. From Figure 3 (a1-2 and b1-2), there is no significant difference stemming from in-situ heating during the coating process, visible from the topographical view and texture. Relatively rough topography with considerable waviness is visible on top surface; Deep comb-shaped features at the vicinity of the hills of bonded particles are a common observation. Although the spherical particles are frequent at the surfaces, some parts are flattened upon the deformation caused by high velocity impacts. Similar roughness parameters were calculated from the texture. Both cold sprayed Al6061 coatings sprayed with and without substrate preheating showed hydrophilic behavior in a way that water droplets tended to continuously spread over the surface in a relatively short amount of time. This phenomenon that took place faster for Al (HP), wetting a larger area of the specimen, might be related to the difference in porosity network and chemistry of the surface. Although the temperature of heated substrate was 200 ± 5 °C before the starting cold spray deposition and surface temperature remained below 100 °C during the cold spray process, the only variants that might have changed the performance were the heating conditions.

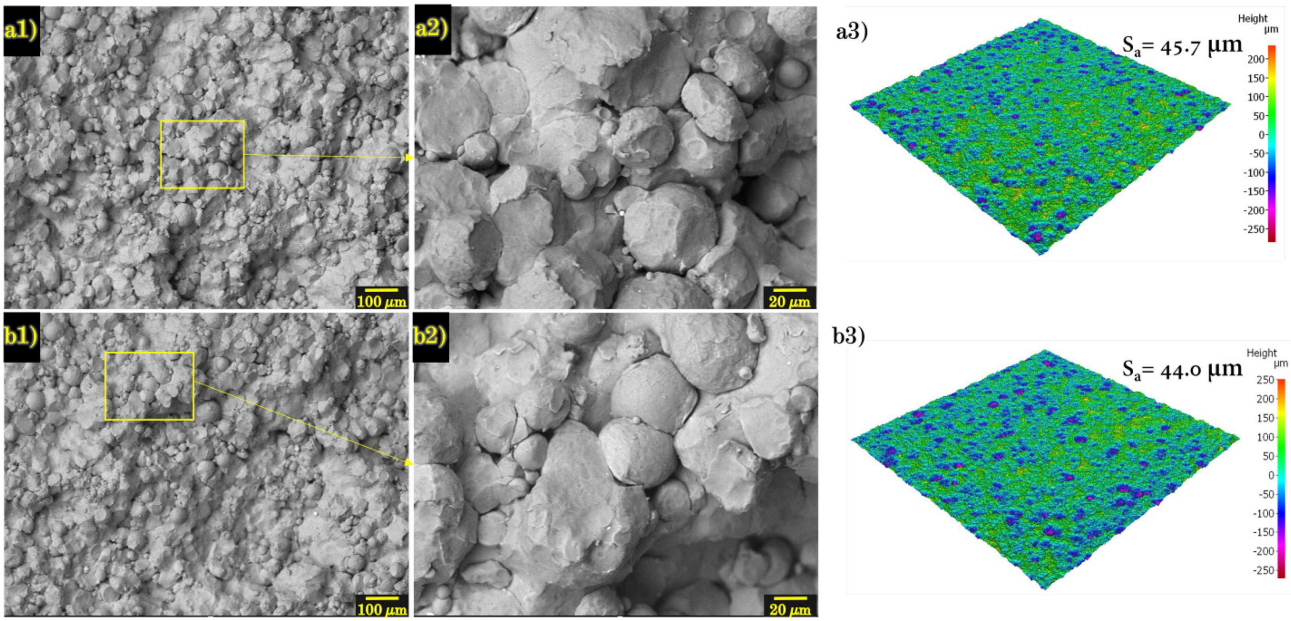

Figure 3. SEM BSE-S topography images and surface texture of cold sprayed a) Al and b) Al (HP) coatings. Designated numbers definition 1: low magnification, 2: higher magnification, 3: texture of the examined 2*2 cm^2 area.

SEM micrographs in Figure 4 represent the formation of QC-Al composite surface where coarse QC particles with heavier mean atomic mass appeared as the bright phases. Low magnification views in Figure 4 (a1 and b1) illustrates a random distribution of QC particles over the surface. In both cases, the volume ratio of QC/Al in the initial feedstock declined over the surface of coatings accordingly due to the rebounding of hard QC powders. Higher magnification micrographs (Figure 4 a2 and b2) show bowl-shaped concavities as large as the coarse QC powders are rebounded area with hammered underneath the material. Material flow at the edges of the concavities can be seen regularly all over the surface. Apparently, Al6061 powders deformation took place easier than QC powders;

consequently, it acts like a binder phase embracing the hard QC particles. At rebounded areas, there are small pieces left over from impacted without attachment. Although rebounded particles contribution to the chemistry of the surfaces is not significant in a way that phase contrast can be seen all over the impacted area, the peening effect of previous particles could be counted as a positive effect in densification in microscale, influential in forming the texture and activation of the surface. The amount of loosely bounded and undeformed spherical powders to the surface is smaller compared to sole Al6061 deposition. Smashed segments that appear brighter in the surrounding darker phase demonstrate the brittle nature of the QC particles and the simultaneous capability of ductile Al6061 powders to preserve the fragmented pieces in the coating. Similar deformation mechanisms are well known in cold spraying of metal matrix composites, where the reinforcing component is made of hard particles, especially ceramics [18]. The large cavities are shown on Al6061 coatings replaced by a smoother surface where the difference between the peaks and valleys is less highlighted. Considering the surface roughness (Sa) values reported in Fig 4 (a3 and b3), lower QC content feedstock Al50-cQC(HP) provided less intense hammering led to a rougher as-sprayed surface. Remarkably, water droplets tend to avoid wetting of both surfaces showing hydrophobic behavior with CA above 140°. Although the content of QC powder (volume fraction on the surface) is smaller for Al50-cQC(HP) compared to Al10-cQC(HP), which was observed in overall scan of the surface, close CA values were observed.

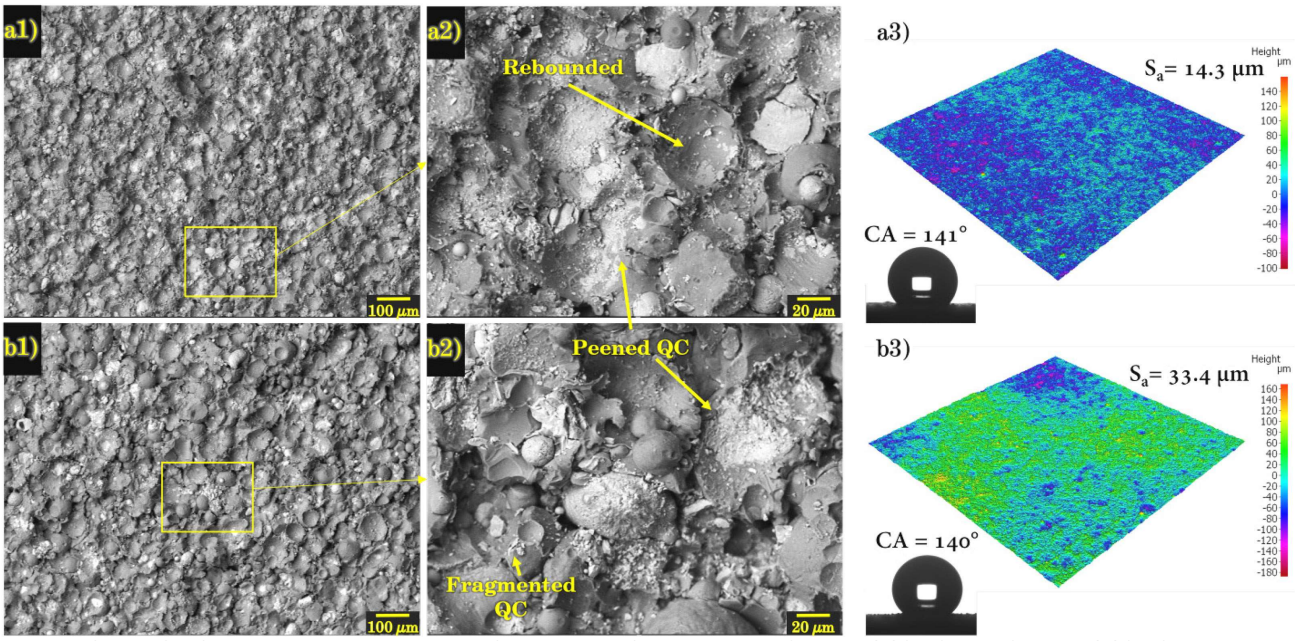

Figure 1. SEM BSE-S topography images and surface texture of cold sprayed a) Al10-cQC(HP) and b) Al50-cQC(HP) coatings. Designated numbers definition 1: low magnification, 2: higher magnification, 3: texture and visualization of contact angle on the examined 2*2 cm^2 area.

Using finer QC particles in the initial powder feedstock mixture revealed a slightly different morphology on the composite surfaces. According to Figure 5 (a1 and b1), the distribution of QC particles over the surfaces are similar with and without substrate heating. Measuring and comparing the relative content of each phase is practically erroneous; apart from the roughness that interferes with image processing, small, scattered fragments of QC powders attached to the soft phase are hard to consider in the image analysis. Smaller in size but higher in number, rebounded zones in Figure 5 (a2 and b2) are visible compared to marks in Figure 4, implying higher fine QC powders rebounding. In the same comparison context, the waviness of the surfaces is more pronounced with deeper concavities and more frequent hills, caused by less intense deformation by smaller QC particles impacts. In accordance with the observation in Figure 4 (a3 and b3), QC particles shifted the wetting behavior from the hydrophilic nature observed in Al6061 coatings to the hydrophobic zone for the composite surfaces. Slightly higher Sa and CA were observed for coating without the heating plate behind the substrate during the process. The roughness reduction can be justified by higher deformation caused by softening induced by the heating. But the change in wetting behavior is more complex to directly correlate to an isolated factor e.g., chemistry or roughness of the surface independently.

Cold sprayed stainless steel (SS316L) surface also showed mechanical bonding the particles upon that impact caused deformation. Therefore, a relatively rough surface was created which shows less deformation from the initial feedstock topography state, conserving the spherical geometry in top view (see Figure 6 (a1 and a2)). Measured contact angle values (Figure 6 (a3)) showed a hydrophilic behavior, similar to several other reports of wettability assessment on coating or bulk SS316L made of other fabrication methods [19,20]. Likewise, Al-QC composite surface, added QC powders in the initial mixture modified the texture of surfaces and chemical composition. As can

be seen in Fig 6 (b1 and b2), the darker QC phases (with lower average atomic mass compared to SS) covered the surface together with SS316L deformed particles. Although this co-deposition led to a slightly smoother surface, the CA measured was more than 2 times higher than that of SS316L metallic coating, leading to a hydrophobic behavior.

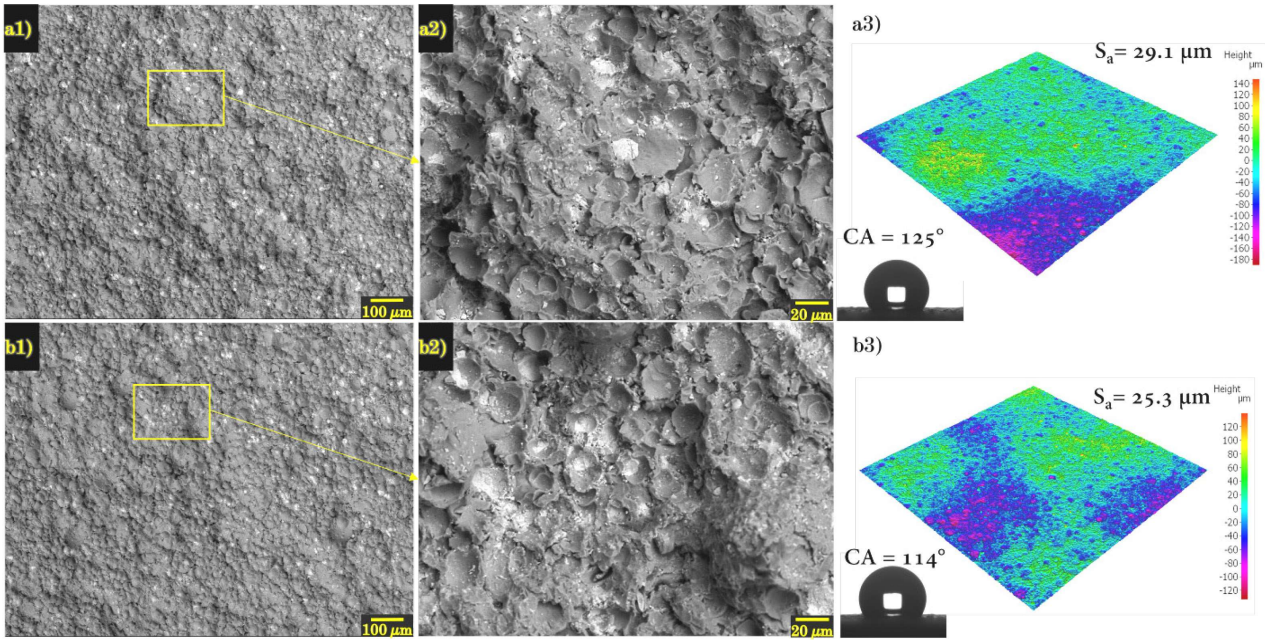

Figure 5. SEM BSE-S topography images and surface texture of cold sprayed a) Al25-fQC and b) Al25-fQC (HP) coatings. Designated numbers definition 1: low magnification, 2: higher magnification, 3: texture and visualization of contact angle on the examined 2*2 cm^2 area.

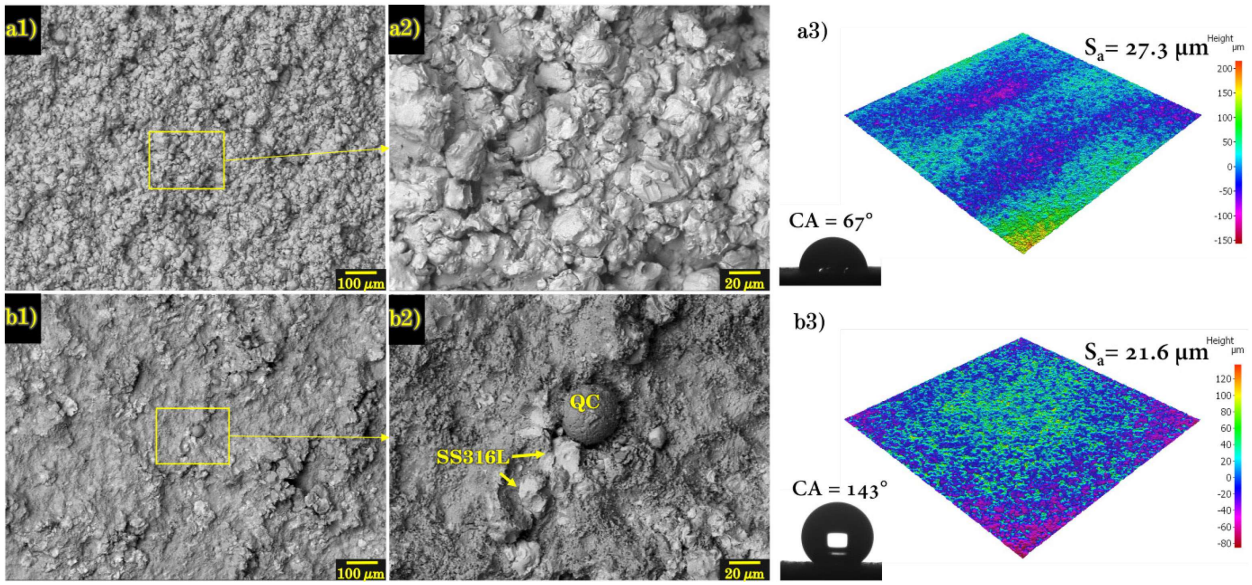

Figure 6. SEM BSE-S topography images and surface texture of cold sprayed a) SS and b) SS25-cQC(HP) coatings. Designated numbers definition 1: low magnification, 2: higher magnification, 3: texture and visualization of contact angle on the examined 2*2 cm^2 area.

4 Discussion

Regarding the exciting applications of hydrophobic/superhydrophobic surfaces, successful trials with versatile spray technologies have been reported in the literature; atmospheric plasma spray of hydroxyapatite containing coatings for biomedical application [19], flame-sprayed polymeric coatings for use in cold regions [21,22], HVOF sprayed wear resistant and hard coatings made of Cr_3C_2-NiCr, WC-Co-Cr [23,24], corrosion resistant Zn and Al-based coatings made by cold spray [25,26] are some of those promising works bringing about multifunctionality to the coating. Generally, two-step processes have been employed to enhance or develop the water repellency by

these methods where post-processing like oil impregnation inside the structure or heat treatment is needed [24,27]. Thus, the idea of having a hydrophobic surface that requires minimal post-processing is very enticing. The motivation behind testing different sets of the coatings in this work was to follow such facile production of durable hydrophobic surfaces, aiming to investigate their performance and see the interaction of process and feedstock variables.

The Al6061 coatings that were made by cold spraying with the same parameter used for Al-QC composite coatings, demonstrated a higher level of porosity. A steady decline in contact angle over time that was observed, might occur due to the water penetration inside pores, as it was observed in HVOF cermet coating with a porous structure [23]. The surface energy of the material also influences water droplet tendency to spread over high energy surfaces or to retain its binding with water molecules and form spherical droplets over low energy surfaces. Comparing to earlier studies [7,8], the gradual disappearance of water droplets over cold sprayed Al6061 coatings in the current study was not surprising.

Unlike the Al6061 coating where higher surface inside the cavities draw water into the pores, the smoother and denser composite coating surfaces did not show the similar behavior. Surface wettability of composites may be altered by changes in surface chemistry or roughness [28]. Presence of low surface energy substances on composites surfaces was found to be influential in modifying the total surface energy, giving rise to water contact angle [29]. Noticing that the presence of Al-QC composite surfaces exhibited increased contact angle might be explained by decreasing the overall surface energy on all of the evaluated composite coatings surfaces. Small QC fragments spread throughout the surface affected the surface energy locally. In Table 2, measured CA values together with surface parameters are also reported. Variation in values can be observed by changing feedstock materials, but in term of surface roughness and texture contribution to the wetting performance, direct conclusion cannot be made.

Table 2. Surface roughness parameters and measured static contact angle values

Sample code	CA (°) ± SD	Calculated surface parameters (primary texture)			
		S_a (µm)	S_q (µm)	S_{Ku}	S_{Ku}
Al	-	44.0	55.8	-0.4	3.4
Al (HP)	-	45.7	57.5	-0.4	3.2
SS	67 ± 7.3	27.3	35.9	0.6	4.8
Al25-fQC	125 ± 3.0	29.1	38.5	-0.5	3.4
Al25-fQC (HP)	114 ± 4.3	25.3	31.4	-0.1	2.9
Al10-cQC	141 ± 2.4	14.3	18.8	0.2	3.7
Al50-cQC(HP)	140 ± 4.3	33.4	42.1	-0.4	3.1
SS25-cQC(HP)	143 ± 0.8	21.6	27.4	0.4	3.2

Comparing with Al6061 cold sprayed surfaces, Al-QC surfaces showed improved hydrophobicity. Nevertheless, the content of QC particles in the initial mixture was not influential as QC particle size was. In general, composites' surfaces composed of coarse QC particles demonstrated a greater hydrophobicity level in both situations of 90 vol. % and 50 vol. % QC particles in the blended feedstock, compared to 75 vol. % fine QC particles in the combination. Cold sprayed Al-QC composite coatings themselves are intriguing because they exhibit enhanced, new, or mixed features in comparison to the properties of their constituents. Other combinations may also exhibit improved hydrophobicity; as a plausible beginning point for these types of studies, a translation toward hydrophobic behavior was seen for a relatively hydrophilic stainless-steel surface -one of the most frequently used materials in structures. While it needs further optimization and analysis, it establishes that cold sprayed composite surfaces with QC particles and altered wetting behavior can be expanded to various alloys as well. Coating mechanical properties, facile methods for mass production, applicability for different purposes and long term stability are some of the challenges in the field [4,5,30]; given that high endurance from cold sprayed Al-QC could be retrieved, it is interesting to extend the functionality and also tackle the other challenges. These findings provide further incentive to conduct application-based research on the extension of this subject.

5 Conclusion

High-pressure cold spray was used to fabricate composite coatings made of Al6061 or stainless steel 316L mixed with quasi-crystalline Al-based powders. The presence of QC particles, in different sizes and content in the cold sprayed metallic composite coatings surfaces, was found a practical approach to change the surface wettability through a one-step process. Alteration from hydrophilic behavior of cold sprayed Al and SS coatings toward hydrophobic behavior in the QC-composite form ($114 < CA° < 140$) owed to the dispersion of low surface energy QC phase over the surface and morphology modification through high-velocity impacts of hard QC particles during cold spray processing. Successful production of hydrophobic cold sprayed metallic-QC composite coatings can open new application areas.

6 Acknowledgement

Authors would like to thank Mr. Jarkko Lehti and Anssi Metsähonkala, of Tampere University, for spraying the coating samples, M.Sc. Jarmo Laakso, of Tampere University, for helping with profilometer studies and Ms. Kaisa Kiuru and Ms. Nastaran Bayat, of Tampere University, for the droplet shape analyses. SEM work made use of Tampere Microscopy Center facilities at Tampere University, Finland. Tampere University, the Faculty of Engineering and Natural Sciences is acknowledged by R.J. for the funding. This research was partly funded by Academy of Finland, project “Thermally Sprayed slippery liquid infused porous surface – towards durable anti-icing coatings” (TS-SLIPS).

7 Literature

[1] J. Drelich, E. Chibowski, D.D. Meng, K. Terpilowski, Hydrophilic and superhydrophilic surfaces and materials, Soft Matter. 7 (2011) 9804–9828. https://doi.org/10.1039/c1sm05849e.

[2] D. Ahmad, I. van den Boogaert, J. Miller, R. Presswell, H. Jouhara, Hydrophilic and hydrophobic materials and their applications, Energy Sources, Part A Recover. Util. Environ. Eff. 40 (2018) 2686–2725. https://doi.org/10.1080/15567036.2018.1511642.

[3] T. Huhtamäki, X. Tian, J.T. Korhonen, R.H.A. Ras, Surface-wetting characterization using contact-angle measurements, Nat. Protoc. 13 (2018) 1521–1538. https://doi.org/10.1038/s41596-018-0003-z.

[4] D. Wang, Q. Sun, M.J. Hokkanen, C. Zhang, F.Y. Lin, Q. Liu, S.P. Zhu, T. Zhou, Q. Chang, B. He, Q. Zhou, L. Chen, Z. Wang, R.H.A. Ras, X. Deng, Design of robust superhydrophobic surfaces, Nature. 582 (2020) 55–59. https://doi.org/10.1038/s41586-020-2331-8.

[5] T. Verho, C. Bower, P. Andrew, S. Franssila, O. Ikkala, R.H.A. Ras, Mechanically Durable Superhydrophobic Surfaces, Adv. Mater. 23 (2011) 673–678. https://doi.org/10.1002/adma.201003129.

[6] J.W. Song, L.W. Fan, Temperature dependence of the contact angle of water: A review of research progress, theoretical understanding, and implications for boiling heat transfer, Adv. Colloid Interface Sci. 288 (2021) 102339. https://doi.org/10.1016/j.cis.2020.102339.

[7] S. Barthwal, Y.S. Kim, S.-H. Lim, Mechanically Robust Superamphiphobic Aluminum Surface with Nanopore-Embedded Microtexture, Langmuir. 29 (2013) 11966–11974. https://doi.org/10.1021/la402600h.

[8] M. Ostapiuk, B. Surowska, J. Bieniaś, Interface analysis of fiber metal laminates, Compos. Interfaces. 21 (2014) 309–318. https://doi.org/10.1080/15685543.2014.854527.

[9] H.R. Sharma, M. Shimoda, A.P. Tsai, Quasicrystal surfaces: Structure and growth of atomic overlayers, Adv. Phys. 56 (2017) 403–464. https://doi.org/10.1080/00018730701269773.

[10] K. Lee, J. Hsu, D. Naugle, H. Liang, Multi-phase quasicrystalline alloys for superior wear resistance, Mater. Des. 108 (2016) 440–447. https://doi.org/10.1016/j.matdes.2016.06.113.

[11] T.P. Yadav, N.K. Mukhopadhyay, Quasicrystal: a low-frictional novel material, Curr. Opin. Chem. Eng. 19 (2018) 163–169. https://doi.org/10.1016/j.coche.2018.03.005.

[12] C.J. Jenks, P.A. Thiel, Quasicrystals: A short review from a surface science perspective, Langmuir. 14 (1998) 1392–1397. https://doi.org/10.1021/la970727+.

[13] J.M. Dubois, E. Belin-Ferré, Wetting and adhesion properties of quasicrystals and complex metallic alloys, Appl. Adhes. Sci. 3 (2015). https://doi.org/10.1186/s40563-015-0046-0.

[14] F.R.P. Feitosa, R.M. Gomes, M.M.R. Silva, S.J.G. De Lima, J.M. Dubois, Effect of oxygen/fuel ratio on the microstructure and properties of HVOF-sprayed Al59Cu25.5Fe12.5B3 quasicrystalline coatings, Surf. Coatings Technol. 353 (2018) 171–178. https://doi.org/10.1016/j.surfcoat.2018.08.081.

[15] J. Kong, C. Zhou, S. Gong, H. Xu, Low-pressure plasma-sprayed Al-Cu-Fe-Cr quasicrystalline coating for Ti-based alloy oxidation protection, Surf. Coatings Technol. 165 (2003) 281–285. https://doi.org/10.1016/S0257-8972(02)00751-X.

[16] H. Assadi, H. Kreye, F. Gärtner, T. Klassen, Cold spraying – A materials perspective, Acta Mater. 116 (2016) 382–407. https://doi.org/10.1016/j.actamat.2016.06.034.

[17] H. Koivuluoto, P. Vuoristo, Effect of Ceramic Particles on Properties of Cold-Sprayed Ni-20Cr+Al2O3 Coatings, J. Therm. Spray Technol. 18 (2009) 555–562. https://doi.org/10.1007/s11666-009-9345-y.

[18] L. He, M. Hassani, A Review of the Mechanical and Tribological Behavior of Cold Spray Metal Matrix Composites, Springer US, 2020. https://doi.org/10.1007/s11666-020-01091-w.

[19] A. Woźniak, M. Staszuk, Ł. Reimann, O. Bialas, Z. Brytan, S. Voinarovych, O. Kyslytsia, S. Kaliuzhnyi, M. Basiaga, M. Admiak, The influence of plasma-sprayed coatings on surface properties and corrosion resistance of 316L stainless steel for possible implant application, Arch. Civ. Mech. Eng. 21 (2021) 148. https://doi.org/10.1007/s43452-021-00297-1.

[20] A.M. Souza, R. Ferreira, G. Barragán, J.G. Nuñez, F.E. Mariani, E.J. da Silva, R.T. Coelho, Effects of Laser Polishing on Surface Characteristics and Wettability of Directed Energy-Deposited 316L Stainless Steel, J. Mater. Eng. Perform. 30 (2021) 6752–6765. https://doi.org/10.1007/s11665-021-05991-y.

[21] H. Koivuluoto, C. Stenroos, M. Kylmälahti, M. Apostol, J. Kiilakoski, P. Vuoristo, Anti-icing Behavior of

Thermally Sprayed Polymer Coatings, J. Therm. Spray Technol. 26 (2017) 150–160. https://doi.org/10.1007/s11666-016-0501-x.
[22] V. Donadei, H. Koivuluoto, E. Sarlin, P. Vuoristo, Icephobic Behaviour and Thermal Stability of Flame-Sprayed Polyethylene Coating: The Effect of Process Parameters, J. Therm. Spray Technol. 29 (2020) 241–254. https://doi.org/10.1007/s11666-019-00947-0.
[23] P. Komarov, D. Jech, S. Tkachenko, K. Slámečka, K. Dvořák, L. Čelko, Wetting Behavior of Wear-Resistant WC-Co-Cr Cermet Coatings Produced by HVOF: The Role of Chemical Composition and Surface Roughness, J. Therm. Spray Technol. 30 (2021) 285–303. https://doi.org/10.1007/s11666-020-01130-6.
[24] D. Jin, Z. Di, K. Pan, M. Xiong, F. Yang, S. Wei, Hydrophobicity of Cr3C2-NiCr coating under mechanical abrasion and thermal annealing, Appl. Surf. Sci. 574 (2022) 151600. https://doi.org/10.1016/j.apsusc.2021.151600.
[25] Y. Wang, M. Wu, P. Lu, W. Zhou, X. Shi, K. Yang, X. Miao, Mechanical and corrosion resistance of cold sprayed zinc (CSZ) nano composite coating enhanced by SiO2-GO hybrid material, Colloids Surfaces A Physicochem. Eng. Asp. 632 (2022) 127824. https://doi.org/10.1016/j.colsurfa.2021.127824.
[26] F.F. Lu, K. Ma, C. xin Li, C. jiu Li, Enhanced Corrosion Resistance of a Double Ceramic Composite Coating Deposited by a Novel Method on Magnesium-Lithium Alloy (LA43M) Substrates, J. Therm. Spray Technol. 30 (2021) 680–693. https://doi.org/10.1007/s11666-020-01143-1.
[27] V. Donadei, H. Koivuluoto, E. Sarlin, P. Vuoristo, Lubricated icephobic coatings prepared by flame spraying with hybrid feedstock injection, Surf. Coatings Technol. 403 (2020) 126396. https://doi.org/10.1016/j.surfcoat.2020.126396.
[28] C. Li, Y. Sun, M. Cheng, S. Sun, S. Hu, Fabrication and characterization of a TiO2/polysiloxane resin composite coating with full-thickness super-hydrophobicity, Chem. Eng. J. 333 (2018) 361–369. https://doi.org/10.1016/j.cej.2017.09.165.
[29] J. Gao, Y. Wu, Z. Zhang, D. Zhao, H. Zhu, K. Xu, Y. Liu, Achieving amorphous micro-nano superhydrophobic structures on quartz glass with a PTFE coating by laser back ablation, Opt. Laser Technol. 149 (2022) 107927. https://doi.org/10.1016/j.optlastec.2022.107927.
[30] A.T. Abdulhussein, G.K. Kannarpady, A.B. Wright, A. Ghosh, A.S. Biris, Current trend in fabrication of complex morphologically tunable superhydrophobic nano scale surfaces, Appl. Surf. Sci. 384 (2016) 311–332. https://doi.org/10.1016/j.apsusc.2016.04.186.